ChemComm

COMMUNICATION

View Article Online
View Journal

Cite this: DOI: 10.1039/d4cc05232c

Received 5th October 2024,
Accepted 20th December 2024

DOI: 10.1039/d4cc05232c

rsc.li/chemcomm

Luminescent terbium(III) probes containing an aromatic amino acid-based antenna for discrimination between adenine and guanine nucleotides†

Sunanda Pradhan, Nitin Shukla, ‡ Goutam Panigrahi ‡ and Ashis K. Patra *

Herein we present a series of luminescent Tb(III)-probes ([Tb-L^{trp}], [Tb-L^{tyr}], and [Tb-L^{phe}]) for sensing and discriminating purine nucleoside polyphosphates (NPP) based on a modified DTTA chelator appended to aromatic amino acids (L^{aa}). The optically most effective luminescent [Tb-L^{trp}] probe preferentially discriminates the guanine-NPPs over the adenine-NPPs *via* PeT-based modulation of Tb(III) luminescence within the biological concentration range.

Nucleoside polyphosphates (NPPs) are important physiological phosphates (PPs) that are vital for energy storage, transfer and consumption, as building blocks in DNA synthesis, phosphorylation, molecular recognition, cellular transduction, and regulation of crucial enzyme activities, and so on.[1,2] Therefore, maintaining a healthy physiological homeostatic range of NPPs for regulating a plethora of intracellular processes is critical for normal cellular functions. Their dysfunction or dysregulation is intimately related to numerous critical life-threatening diseases like hypoparathyroidism, metabolic and respiratory acidolysis, chronic kidney diseases, cancers, *etc.*[3] Therefore, designing sensitive and selective probes to monitor the level of various NPPs and differentiating them under physiological conditions are of immense importance in drug discovery, diagnostic medicine and disease management.[4,5] The discrimination of such NPPs is highly challenging owing to their structural similarity, similar ionic charge, and pH-dependent configurations.[6] Furthermore, the concentration of these individual NPPs is much lower compared to other abundant physiological anions in the blood (*e.g.*, HCO_3^-: 23–29 mM; Cl^-: 98–105 mM; lactate: 0.5–1 mM).[7] Consequently, the probes having high sensitivity to detect NPPs in biological environments are very limited. Even though some organic fluorescent assays are reported[6] and are being used, they lack desirable selectivity, are expensive, require complex instrumentation, and can only be used for end-point detection.[8] The recognition of physiological phosphates in water depends mainly on electrostatic/H-bonding interactions; however, most organic receptors interacting with these weak intermolecular forces are inadequate to compensate for the high hydration enthalpy barrier of phosphate groups and are thus unsuitable in aqueous media.[2] Thoughtfully designed luminescent lanthanide(III)-based molecular receptors have great potential for recognizing nucleoside polyphosphates under physiological conditions. The emissive Ln(III) probes offer unrivaled and distinctly advantageous optical properties for sensing, bioimaging or real-time monitoring of biologically important anions. The Ln(III) probes possess long luminescence lifetime, sharp emission bands in Vis-NIR, large pseudo-Stokes shift, resistance to photobleaching, *etc.*, which are valuable prerequisites for highly sensitive bioresponsive luminescent probes.[8] The longer lifetime (τ, μs–ms) permitting time-resolved luminescence (TRL) assay without short-lived biological autofluorescence is ideal for achieving a higher S/N ratio with higher sensitivity for *in situ* real-time monitoring under physiological conditions. The affinity and selective recognition could be achieved by structural and conformational modulation of the probes.[8,9] In addition to non-covalent interactions for enhanced selectivity for structurally comparable NPPs, the hard Ln(III) ions provide strong ionic bonding with hard PO_4^{3-} over organic probes to overcome high $\Delta G_{hydration}$ in a competitive environment.[2] Due to their distinct binding modes and simultaneous disruption of the ET pathways *via* modulation of the antenna effect to excite Ln(III), targeted Ln(III)-molecular receptors interact with nucleotides to produce varied degrees of TRL intensity changes as well as the intended discrimination.

A careful design of the chelating antenna with potential non-covalent interaction sites allows further fine-tuning of selectivity and sensitivity for targeted NPPs based on their structural differences, overall charge, and steric constraints at the labile open coordination sites *via* non-covalent interactions (H-bonding, π–π stacking, *etc.*).[9] Such outer-sphere binding interaction is also an effective strategy for the selective detection of NPPs to minimize the risk of hydrolysis and ligand exchange/displacement with the

Department of Chemistry, Indian Institute of Technology Kanpur, Uttar Pradesh 208016, India. E-mail: akpatra@iitk.ac.in

† Electronic supplementary information (ESI) available. See DOI: https://doi.org/10.1039/d4cc05232c

‡ Contributed equally.

target analytes.[10] Butler *et al.* systematically developed a series of quinoline-appended macrocyclic Eu(III) probes, evaluated their binding affinity and discrimination to various NPPs, and ultimately utilized them for real-time monitoring of kinase activity and inhibitor assays.[11] Such secondary interaction could result in the formation of Ln(III)probe-NPP ternary systems and trigger alternative energy transfer pathways (*e.g.*, PeT), perturbing the ET to Ln(III) and its TRL-intensity.[12] These properties were well tailored by Pierre's group using a phenanthridine-based Tb(III) probe, [Tb-DOTAm-Phen]$^{3+}$, that can selectively detect and discriminate ATP and GTP in the presence of ADP/AMP or GDP/GMP in aqueous media *via* favorable π–π stacking interaction that promotes PeT which prevents the ET to Tb(III), subsequently quenching TRL intensity.[10a,b] The guanine nucleotides are engaged in guanine nucleotide-binding proteins regulated by GTPases, and control critical biological functions like protein synthesis, cell growth, differentiation and signaling.[13] The RAS proteins are small GTPases that tightly regulate the signaling, cell growth, differentiation, and mutations associated with cancers by acting as a binary switch in a GTP/GDP-bound state.[14] Moreover, G-nucleotides are associated with GPCR, a pivotal drug target, and play important roles in numerous cellular signal transduction processes.[15] The conversion of GDP to GTP is a crucial step in the Krebs cycle and GTP is also necessary in the gluconeogenesis process.[16] Therefore, designing sensitive optical probes for selective detection and real-time monitoring of G-NPPs under physiological conditions is crucial for studying a plethora of biochemical processes, drug discovery, and diagnosis.

Herein, we report three water-soluble luminescent and structurally related Tb(III)-complexes ([**Tb-L^{aa}**]: [**Tb-L^{trp}**], [**Tb-L^{tyr}**], and [**Tb-L^{phe}**]) based on a modified polyaminocarboxylate DTTA-chelator appended to aromatic amino acids (*i.e.*, L-trp, L-tyr, and L-phe) as a potential sensitizing antenna (**L^{aa}**) (Fig. 1) that can discriminate between the guanine (G) and adenine (A) purine bases and their corresponding nucleoside phosphates. Through strong Tb^{3+}–COO^- ionic interactions, the four carboxylate arms of DTTA–CO_2Me form a strong chelating environment around the hard Tb(III), enhancing both thermodynamic and kinetic stability. Such strong multidentate chelation prevents leaching out of Tb(III) ions and allows the probe to be used in competitive aqueous biological media.

The carboxylate arm of the appended amino acid was esterified to prevent high anion–anion repulsion between the NPP anions and the Tb(III) probes. The aromatic side chains of the bioessential amino acids were meticulously chosen as potential sensitizing antennae that can facilitate the efficient energy transfer (ET) to Tb(III)*, while making the [**Tb-L^{aa}**] probes more biocompatible as desired in the physiological media. Additionally, the aromatic side chains in these amino acids allow favorable non-covalent π–π-stacking interactions with the nucleobases for selective recognition and possibly affect the ET-pathways to sensitize the Tb(III) ion *via* triggering the PeT process. The effective antenna effect of the conjugated tryptophan results in stronger luminescence for [**Tb-L^{trp}**] compared to the other two congeners ([**Tb-L^{tyr}**] and [**Tb-L^{phe}**]), and therefore, it is selected for a systematic study as a time-resolved luminescent probe for discriminating purine nucleoside phosphates. Under controlled physiological conditions (10 mM HEPES, pH 7.2), the [**Tb-L^{trp}**] probe can selectively differentiate between guanine and adenine nucleotides even in the presence of other biologically relevant anions. A detailed investigation led us to predict that the non-covalent π–π stacking interaction operating between the extended indole ring of L-trp in the [**Tb-L^{trp}**] probe and the guanine base promotes PeT from the HOMO of guanine to the excited indole ring causing non-radiative quenching of the luminescence intensity (Fig. 2). This work is among the very few luminescent Tb(III) probes that can differentiate between two purine nucleotides with high selectivity for guanine NPPs.

The aromatic amino acid containing DTTA-chelates (**L^{trp}**, **L^{phe}**, **L^{tyr}**) were prepared using a multi-step synthesis and characterized (Fig. S1–S20, ESI†). The [**Tb-L^{aa}**] probes were synthesized from the reaction of $TbCl_3{\cdot}6H_2O$ with base-neutralized **L^{aa}** ligands (details in the ESI†). The aromatic side chains of the amino acids were used as a sensitizing antenna *via* efficient ET to excite Tb(III) to exhibit long-lived green luminescence as a valuable tool for sensing physiological phosphates in biological media. Moreover, the [**Tb-L^{aa}**] receptors bind to NPPs through weaker non-covalent π–π-stacking interactions between these aromatic antennae and the purine bases of the nucleotides. The UV-vis spectral profile of [**Tb-L^{aa}**] in the HEPES buffer shows ligand-centered $\pi \rightarrow \pi^*/n \rightarrow \pi^*$ transitions without much perturbation from the free antennae (**L^{aa}**) when complexed with Tb(III) (Fig. S21, ESI†).

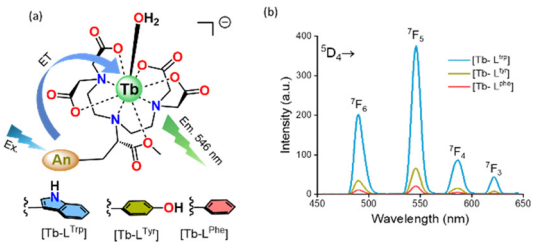

Fig. 1 (a) Proposed structures of [**Tb-L^{aa}**] (**L^{aa}** = **L^{trp}**, **L^{tyr}**, **L^{phe}**) showing the ET-pathways. (b) Time-resolved luminescence spectra of [**Tb-L^{aa}**] complexes: [**Tb-L^{trp}**], [**Tb-L^{tyr}**], [**Tb-L^{phe}**] showing respective $^5D_4 \rightarrow {}^7F_J$ transitions. Conditions: [**Tb-L^{aa}**] = 25 μM in 10 mM HEPES buffer (pH 7.2), λ_{ex} = 290 nm (**Tb-L^{trp}**), 278 nm (**Tb-L^{tyr}**), and 260 nm (**Tb-L^{phe}**), ex./em. slit width = 5 nm, delay and gate time = 0.5 ms, T = 298 K.

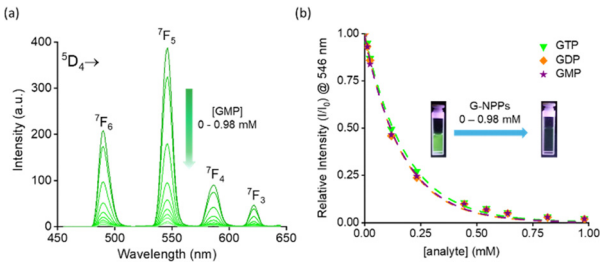

Fig. 2 Time-resolved luminescence spectra of [**Tb-L^{trp}**]. (a) Decrease in the emission intensity upon the addition of GMP (0–0.98 mM). (b) Relative changes of $^5D_4 \rightarrow {}^7F_5$ emission peak intensity (I/I_0) at 546 nm *vs.* concentration of G-NPPs (0–0.98 mM). Conditions: [**Tb-L^{trp}**] = 25 μM, 10 mM HEPES buffer (pH 7.2), λ_{ex} = 290 nm, ex./em. slit width = 5 nm, delay and gate time = 0.5 ms, T = 298 K.

This observation suggests predominant ionic bonding between the Tb(III) and anionic $[\mathbf{L^{aa}}]^{4-}$ ligands without any ligand field effect and non-participation of the deeply shielded 4f-orbitals of Tb(III) in bonding. The TRL spectra for [**Tb-L^{aa}**] probes in HEPES buffer (10 mM, pH 7.2) show characteristic sharp emissions originating from $^5D_4 \rightarrow {}^7F_J$ transitions of Tb(III) (Fig. S22, ESI†). The Tb(III) luminescence intensity follows the order [**Tb-L^{trp}**] > [**Tb-L^{tyr}**] > [**Tb-L^{phe}**] linked to the relative trends in the photosensitization and ET-efficacy of the corresponding antenna moieties. The more intense time-delayed luminescence from the [**Tb-L^{trp}**] probe was ideally used for in-depth interaction studies with various NPPs, nucleobases and other anions. The excited-state lifetimes of the luminescent [**Tb-L^{aa}**] probes ranging from 0.4 to 1.7 ms enable time-gated detection of various purine NPPs with higher S/N ratios in aqueous buffer media. In particular, the continuous addition of guanine nucleotides (GMP, GDP, GTP, 0 to 0.98 mM) results in near complete quenching (~98%) of the emission intensity of the [**Tb-L^{trp}**] probe measured at 546 nm ($^5D_4 \rightarrow {}^7F_5$) (Fig. 3a). Adding various adenine nucleosides, nucleotides and free bases results in relatively much less luminescence quenching (20–30%) for the $\Delta J = 1$ band ($^5D_4 \rightarrow {}^7F_5$). However, the probe was unable to show any discernible differentiation within the guanosine mono-, di- and tri-phosphates presumably due to identical stacking interactions between the **L^{trp}** and guanine bases. Overall, the [**Tb-L^{trp}**] probe collectively showed significant selective discrimination for the guanine-based NPPs over their adenine analogs (Fig. 3a). Moreover, the [**Tb-L^{trp}**] probe was able to detect the presence of guanine-based nucleotides even in the presence of excess of corresponding adenine nucleotides (Fig. 3b). Such selective discrimination of guanine NPPs could be potentially due to the higher energy of the HOMO compared to adenine for efficient PeT quenching with the indole moiety of **L^{trp}**. Such selectivity for guanine nucleotides will be of potential utility for continuous monitoring of various enzymatic activities or inhibitor screening by measuring guanine NPPs in real-time.[10b] The selectivity and interference studies with various biologically abundant anions with GMP in HEPES buffer reveal no apparent interference with the selectivity of [**Tb-L^{trp}**] for guanine nucleotides underscoring its utility in complex biological media (Fig. S24, ESI†).

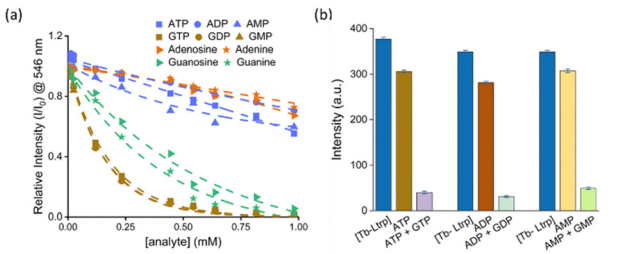

Fig. 3 (a) Relative changes of $^5D_4 \rightarrow {}^7F_5$ emission peak intensity (I/I_0) for [**Tb-L^{trp}**] at 546 nm *vs.* concentrations of various NPPs and nucleobases (C = 0–0.98 mM). (b) Bar diagram showing the selective and significant quenching of [**Tb-L^{trp}**] luminescence intensity by G-NPPs in the presence of corresponding A-NPPs. Conditions: [**Tb-L^{trp}**] = 25 μM in HEPES buffer (10 mM, pH 7.2), [A-NPPs] and [G-NPPs] = 0.64 mM, λ_{ex} = 290 nm, ex./em. slit width = 5 nm, delay and gate time = 0.5 ms, T = 298 K.

The hydration number (q) of the probe was determined from the τ_{H_2O} and τ_{D_2O} using modified Horrock's equation to gain insight into the molecular interactions of the [**Tb-L^{trp}**] probe with various purine NPPs (ESI†).[17] The $q \approx 1$ was observed before and after the addition of various mono-/di-/tri-nucleoside polyphosphates. This suggests only the presence of weaker electrostatic interactions and no direct coordination of the phosphate with Tb(III) *via* displacement of bound H_2O, but the NPPs essentially remained in the vicinity by stacking with the purine bases (Table S1 and Fig. S25, ESI†). Notably, the absence of such direct coordination of phosphates in NPPs to the Tb(III) ion in $[\text{Tb-DOTAm-phen}]^{3+}$ was also reported by Perrie *et al.*[10b] This result also pertains to non-discrimination of various G-NPPs with [**Tb-L^{trp}**], while having different negative charge densities. Therefore, the Tb(III) emission quenching primarily originated from the relatively weaker but favorable hydrophobic π–π stacking of the planar indole ring and guanine bases. To probe these interactions further, we performed individual TRL and fluorescence titrations of various A/G bases, nucleosides and nucleotides with the [**Tb-L^{trp}**] probe (Fig. 3a) and free **L^{trp}** antenna (Fig. S23, ESI†). We observed distinctly significant quenching in the emission intensity with guanine-NPPs compared to their adenine counterparts. These findings augment the preferential interactions between guanine and indole moiety in the **L^{trp}** ligand and the [**Tb-L^{trp}**] probe. The efficient quenching of the **L^{trp}** antenna's luminescence strongly indicates the involvement of PeT from the purine bases to indole, preventing ET to Tb(III), thereby quenching Tb(III) emission.

We observed similar trends in the PeT-based luminescence quenching for [**Tb-L^{tyr}**] and [**Tb-L^{phe}**] with purine NPPs, but with inadequate discrimination for A/G-nucleotides (Fig. S26 and S27, ESI†). This could be explained by relatively weaker π–π stacking between the less extended planar Ph/Ph-OH moieties and guanine bases resulting in relatively poor PeT quenching and/or involvement of unfavorable excited state energy levels for an effective PeT. The literature reports also suggest a higher HOMO energy level of guanine over adenine bases for effective PeT.[18] This forms an optimal energy gap that promotes efficient PeT from the guanine-based HOMO to the indole-based singlet excited state in **L^{trp}**. Therefore, it prevents further ET to Tb(III), resulting in luminescence quenching of the [**Tb-L^{trp}**] probe. However, a relatively lower HOMO level of adenine makes the PeT to indole less efficient with possible thermal back energy transfer and, thereby, weaker quenching of [**Tb-L^{trp}**] in the presence of adenine NPPs over guanine analogs. The Stern–Volmer quenching constants were determined from the TRL-titration of [**Tb-L^{trp}**] with all six A/G-nucleotides (Fig. S28, ESI†). The guanine nucleotides showed distinctly higher K_{SV} (9.12–13.14 mM^{-1}) *vs.* adenine nucleotides (0.65–0.7 mM^{-1}), ideal for their efficient discrimination in physiological media. The K_{SV} values for G-NPPs were within the physiological mM concentration ranges of the NPPs. The lower K_{SV} values also indicate the absence of any direct coordination of phosphate to Tb(III), and relatively weaker π–π stacking prevails between the indole ring and the guanine bases. This brings [**Tb-L^{trp}**] and G-NPPs in close vicinity for synergistically promoting an efficient PeT and

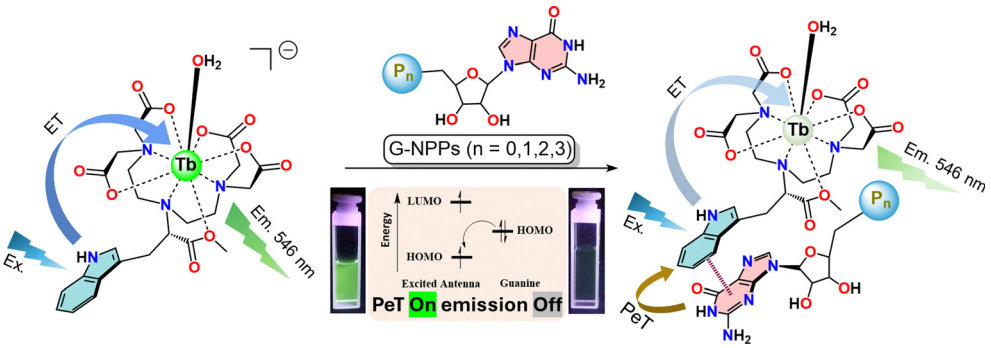

Fig. 4 Proposed mechanism of interaction of guanine NPPs with [**Tb-L^{trp}**] and quenching of TRL due to the PeT process. The weak π–π stacking between the indole moiety and guanine promotes the PeT resulting in a decrease in ET to Tb(III) and its luminescence quenching. A sharp decrease in green emission intensity of [**Tb-L^{trp}**] upon the addition of GMP is visualized by the naked eye upon irradiation with a UV lamp (λ_{irr} = 254 nm).

suppressing the ET to Tb(III) and hence quenching its luminescence intensity as depicted in the proposed mechanism in Fig. 4. Here, the operative PeT switch at the indole antenna moiety with guanine reduces the sensitizing ability *via* ET to populate the emissive $^5D_4$ state and quenches the TRL intensity. Possibly due to such indirect modulation of PeT quenching on intricate ET pathways at a distant recognition site, τ_{Tb} in [**Tb-L^{trp}**] from the decay of $^5D_4 \rightarrow {}^7F_5$ transitions remains unaffected.[10,12,19] This is also accompanied by only minimal disruption at the first coordination sphere of Tb(III) in the absence of direct coordination of phosphates with Tb(III), resulting in comparable deactivation pathways. The limit of detection for G-NPPs calculated from the TRL response of [**Tb-L^{trp}**] was ~1–2 ppm (Fig. S29 and Table S2, ESI†).

In conclusion, we designed three water-soluble, thermodynamically stable and structurally related luminescent Tb(III) probes, *viz.* [**Tb-L^{trp}**], [**Tb-L^{tyr}**], and [**Tb-L^{phe}**] with an octadentate DTTA-chelator conjugated to aromatic amino acids as antennae. The superior [**Tb-L^{trp}**] emerged as an efficient TRL probe that can readily differentiate between the guanine nucleotides over adenine congeners *via* quenching of Tb(III) luminescence involving efficient PeT from weak non-covalent π–π-stacking interactions between the planar guanine base and the indole ring. Further studies with other physiological phosphates are ongoing. The [**Tb-L^{trp}**] probe is a promising choice for real-time monitoring of guanine-based physiological phosphates in biochemical pathways.

A. K. P. thanks the Science and Engineering Research Board (SERB) for the financial support (CRG/2021/000527). S. P. acknowledges UGC for a fellowship, N. S. acknowledges CSIR for a fellowship and G. P. acknowledges Prime Minister's Research Fellowship (PMRF), India for a fellowship.

Data availability

The data supporting this article have been included as part of the ESI.†

Conflicts of interest

There are no conflicts to declare.

Notes and references

1 (*a*) Y. Zhou, Z. Xu and J. Yoon, *Chem. Soc. Rev.*, 2011, **40**, 2222–2235; (*b*) A. M. Agafontsev, A. Ravi, T. A. Shumilova, A. S. Oshchepkov and E. A. Kataev, *Chem. – Eur. J.*, 2019, **25**, 2684–2694.
2 (*a*) M. V. Ramakrishnam Raju, S. M. Harris and V. C. Pierre, *Chem. Soc. Rev.*, 2020, **49**, 1090–1108; (*b*) T. L. M. Martinon and V. C. Pierre, *Chem. – Asian J.*, 2002, **17**, e202200495.
3 M. Rroji, A. Figurek, D. Viggiano, G. Capasso and G. Spasovski, *Int. J. Mol. Sci.*, 2022, **23**, 7362–7378.
4 A. Akdeniz, M. G. Caglayan, I. Polivina and P. Anzenbacher, *Org. Biomol. Chem.*, 2016, **14**, 7459–7462.
5 T. Sakamoto, A. Ojida and I. Hamachi, *Chem. Commun.*, 2009, 141–152.
6 A. E. Hargrove, S. Nieto, T. Zhang, J. L. Sessler and E. V. Anslyn, *Chem. Rev.*, 2011, **111**, 6603–6782.
7 S. J. Butler and D. Parker, *Chem. Soc. Rev.*, 2013, **42**, 1652–1666.
8 (*a*) D. Parker, J. D. Fradgley and K.-L. Wong, *Chem. Soc. Rev.*, 2021, **50**, 8193–8213; (*b*) M. C. Heffern, L. M. Matosziuk and T. J. Meade, *Chem. Rev.*, 2014, **114**, 4496–4539; (*c*) J. C. Bünzli, *Coord. Chem. Rev.*, 2015, **293–294**, 19–47; (*d*) K. Singh, S. Singh, P. Srivastava, S. Sivakumar and A. K. Patra, *Chem. Commun.*, 2017, **53**, 6144–6147; (*e*) K. Gupta and A. K. Patra, *ACS Sens.*, 2020, **5**, 1268–1272.
9 (*a*) S. E. Bodman and S. J. Butler, *Chem. Sci.*, 2021, **12**, 2716–2734; (*b*) S. H. Hewitt, G. Macey, R. Mailhot, M. R. J. Elsegood, F. Duarte, A. M. Kenwright and S. J. Butler, *Chem. Sci.*, 2020, **11**, 3619–3628; (*c*) S.-Y. Huang, M. Qian and V. C. Pierre, *Inorg. Chem.*, 2020, **59**, 4096–4108; (*d*) M. L. Aulsebrook, M. Starck, M. R. Grace, B. Graham, P. Thordarson, R. Pal and K. L. Tuck, *Inorg. Chem.*, 2018, **58**, 495–505; (*e*) L. J. Charbonnière, R. Schurhammer, S. Mameri, G. Wipff and R. F. Ziessel, *Inorg. Chem.*, 2005, **44**, 7151–7160.
10 (*a*) E. A. Weitz, J. Y. Chang, A. H. Rosenfield and V. C. Pierre, *J. Am. Chem. Soc.*, 2012, **134**, 16099–16102; (*b*) E. A. Weitz, J. Y. Chang, A. H. Rosenfield, E. A. Morrow and V. C. Pierre, *Chem. Sci.*, 2013, **4**, 4052–4060; (*c*) X. Liu, J. Xu, Y. Lv, W. Wu, W. Liu and Y. Tang, *Dalton Trans.*, 2013, **42**, 9840–9846.
11 (*a*) S. H. Hewitt, R. Ali, R. Mailhot, C. R. Antonen, C. A. Dodson and S. J. Butler, *Chem. Sci.*, 2019, **10**, 5373–5381; (*b*) S. H. Hewitt, J. Parris, R. Mailhot and S. J. Butler, *Chem. Commun.*, 2017, **53**, 12626–12629.
12 T. Terai, K. Kikuchi, S.-Y. Iwasawa, T. Kawabe, Y. Hirata, Y. Urano and T. Nagano, *J. Am. Chem. Soc.*, 2006, **128**, 6938–6946.
13 I. R. Vetter and A. Wittinghofer, *Science*, 2001, **294**, 1299–1304.
14 D. K. Simanshu, D. V. Nissley and F. McCormick, *Cell*, 2017, **170**, 17–33.
15 A. S. Hauser, M. M. Attwood, M. Rask-Andersen, H. B. Schiöth and D. E. Gloriam, *Nat. Rev. Drug Discovery*, 2017, **16**, 829–842.
16 P. Rogne, B. Dulko-Smith, J. Goodman, M. Rosselin, C. Grundström, C. Hedberg, K. Nam, A. E. Sauer-Eriksson and M. Wolf-Watz, *Biochemistry*, 2020, **59**, 3570–3581.
17 W. D. Horrocks, Jr. and D. R. Sudnick, *J. Am. Chem. Soc.*, 1979, **101**, 334–340.
18 B. Pullman and A. Pullman, *Proc. Natl. Acad. Sci. U. S. A.*, 1958, **44**, 1197–1202.
19 P. A. Tanner, L. Zhou, C. Duan and K.-L. Wong, *Chem. Soc. Rev.*, 2018, **47**, 5234–5265.

